Phys. JETP 34, 906 (1972)].
[9]L. G. Aslamazov and A. I. Larkin, Zh. Eksp. Teor. Fiz. 68, 766 (1975) [Sov. Phys. JETP 41, 381 (1975)].
[10]L. T. Koldaeva, G. P. Motulevich, and A. A. Shubin, Kratk. Soobshch. Fiz. No. 3, 36 (1977).
[11]R. Y. Chiao, M. J. Feldman, H. Ohta, and P. T. Parrish, Rev. Phys. Appl. 9, 183 (1974).
[12]P. W. Anderson and A. H. Dayem, Phys. Rev. Lett. 13, 195 (1964).
[13]M. A. Janocko, J. R. Gavaler, and C. K. Jones, IEEE Trans. Magn. MAG-11, 880 (1975).
[14]A. I. Golovashkin, I. S. Levchenko, and A. N. Lykov, Fiz. Tverd. Tela (Leningrad) 18, 3642 (1976) [Sov. Phys. Solid State 18, 2121 (1976)].
[15]P. de Gennes, Superconductivity of Metals and Alloys, Benjamin, New York, 1965 (Russ. Transl., Mir, 1968).
[16]A. J. Dahm, A. Denenstein, D. N. Langenberg, W. H. Parker, D. Rogovin, and D. J. Scalapino, Phys. Rev. Lett, 22, 1416 (1969).

Translated by A. K. Agyei

Multiple Sondheimer oscillations in tungsten plates with atomically pure surfaces

A. M. Grishin, P. P. Lutsishin, Yu. S. Ostroukhov, and O. A. Panchenko

Donetsk Physicotechnical Institute, Ukrainian Academy of Sciences and Physics Institute, Ukrainian Academy of Sciences
(Submitted 12 September 1978)
Zh. Eksp. Teor. Fiz. 76, 1325–1341 (April 1979)

Multiple Sondheimer oscillations (with periods $\Delta H_s = \Delta H_1/s$, $s = 2, 3, 4$) of the magnetoresistance of tungsten plates in a magnetic field $\mathbf{H}\|[100]$ perpendicular to the surfaces are investigated theoretically and experimentally. These oscillations are due to the multiple passage, through the sample thickness, of the electron reflected from the boundaries. The amplitude of the multiple harmonics depends on the electron scattering in the volume and on the character of its reflection from the metal surface. A Fourier analysis of the Sondheimer-signal spectrum and the results of the theoretical analysis, expressed in the form of simple relations, make it possible to determine the mean free path and the specularity coefficients on an atomically pure crystal surface and on a surface sputtered to saturation. The Sondheimer effect is due to the carrier of section A of the hole octahedron of the tungsten Fermi surface.

PACS numbers: 72.15.Gd

1. INTRODUCTION

1. Interest in condensed-state physics phenomena that occur near the surface of a conducting solid or on the surface iteslf has increased recently. Since very pure materials have now become available, and new methods of purifying and obtaining controllable changes in the surface state have been developed, definite progress was made towards the solution of this problem (see, e.g. Ref. 1). This has been helped to a considerable degree by the use of methods of static and radio-frequency size effects. The point is that macroscopic properties of thin samples with dimensions smaller than the electron mean free path l are determined mainly by the scattering of the electrons from the surface. This means that the experimentally measured characteristics (dc resistance, surface impedance, etc.) contain much information on the surface mechanisms of scattering electrons, on the state of the crystal near the boundary, and so on.

2. Consider, for example, a plane-parallel plate of thickness d, placed in a magnetic field H perpendicular to the surface. In a strong magnetic field, when the cyclotron frequency Ω is much higher than the frequency ν of the collisions of the electrons with the scatterers in the volume,

$$\gamma = \nu/\Omega \ll 1, \tag{1.1}$$

the diagonal components of the tensor of the transverse conductivity of the metal are of the order of $\sigma_0\gamma^2$. Here $\sigma_0 \approx ne^2/m\nu$ is the conductivity of the bulk sample in the absence of a magnetic field; $n, -e$, and m are respectively the concentration, charge, and effective mass of the conduction electrons.

The conductivity of a plate with thickness $d \lesssim l$ can differ significantly from $\sigma_0\gamma^2$ in the case of nonspecular reflection of the electrons from the surface. The reason is that in the plate the role of l is assumed by the effective mean free path

$$l_{\text{eff}}^{-1} = l^{-1} + (2d)^{-1}[(1-\rho_0)+(1-\rho_d)].$$

The collisions of the electrons with the boundary are taken into account here phenomenologically, with the aid of a macroscopic characteristic of the metal surface—the specularity coefficient ρ, $0 \leq \rho \leq 1$. The second term in l_{eff}^{-1} is the reciprocal mean free path, in which the electron experiences diffuse scattering from the upper side of the plate with probability $1-\rho_0$ and from the lower side with probability $1-\rho_d$. Therefore the conductivity component that depends monotonically on H is given by

 0038-5646/79/040673-10$02.40

$$\sigma_{mon}\sim\sigma_0\gamma^2\left[1+\frac{l}{d}\left(1-\frac{\rho_0+\rho_d}{2}\right)\right]. \quad (1.2)$$

Just as in an unbounded metal, $\sigma_{mon}\propto H^{-2}$, but it becomes dependent on the thickness d and on the character of the reflection of the electrons from the metal boundary. Figure 1 shows the experimental dependence of the diagonal component of the magnetoresistance for $R_{xx}\approx\sigma_{mon}^{-1}$ on H in tungsten in which both surfaces of the crystal are either both "pure" or both "dirty" (for details see below). It is seen that the resistance decreases when the difuseness of the electron reflection increases. The law $R_{xx}\propto H^2$ is valid in both cases.

3. In addition to the monotonic dependence on the magnetic field, the transverse conductivity experiences periodic changes with small amplitude as a function of H. They lead to the magnetoresistance oscillations of first predicted by Sondheimer.[2] This phenomenon is due to the fact that in a magnetic field the electron-velocity vector transverse to H rotates with frequency Ω. During the time of flight of the electron from one side of the plate to the other, which equals $d/|\bar{v}_z|$, the vector $\mathbf{v}_\perp$ rotates through an angle

$$\xi=\Omega d/|\bar{v}_z|. \quad (1.3)$$

Here v_c and $\mathbf{v}_\perp$ are the longitudinal and transverse electron velocities, $\mathbf{H}\|z$, and the superior bar denotes averaging over the cyclotron period.

Depending on $\bar{v}_z$, the angle ξ changes from very large values ($v_z\to 0$) to a minimum value corresponding to electrons with the maximum possible velocity along the vector H. This group of particles turns out to be special. It is located in the vicinities of the turning points of the Fermi surface and causes the Sondheimer effect.[2] Gurevich[3] has called attention to the fact that in metals with complex Fermi surfaces the most effective among all the electrons are those for which the angle ξ has an extremum. It is easily seen that these electrons be long to the intersectionsof the Fermi surface by the plane $p_z=\text{const}$ with extremal value of the derivative $\partial S/\partial p_z$ is the intersection area and p_z is the momentum of the electron along H, and for these electrons we have

$$\xi_*=2\pi\left|\frac{\partial S_*}{\partial p_z}\right|^{-1}\frac{deH}{c}. \quad (1.3')$$

The relative number of effective electrons can be easily estimated from the condition

$$\delta p_z/p_F\lesssim(v_F/d\Omega)^{1/2}, \quad (1.4)$$

which is obtained under the condition that the scatter of the angle ξ near ξ_* must not exceed π. Here and hereafter an asterisk labels a quantity taken on a section with an extremum of the derivative $\partial S/\partial p_z$.

Finite rotation of the vector $\mathbf{v}_\perp$ relative to an external electric field E leads to the appearance of an exponential factor $\exp(i\xi_*)$ in the oscillating part of the conductivity σ_{osc}. It is now easy to obtain an estimate of σ_{osc}. The latter is proportional to the "surface" part of σ_{mon}, which is already taken into account in (1.2), to the number of effective electrons (1.4), and to the conditional probability of diffuse scattering of the electrons from both sides of the plate with the assumption that they move in the volume of the sample without collisions. In other words

$$\sigma_{osc}\sim\sigma_0\gamma^2\frac{l}{d}\left(\frac{v_F}{d\Omega}\right)^{1/2}\times(1-\rho_0)(1-\rho_d)e^{-d/l_*}e^{i\xi_*}. \quad (1.5)$$

The real and imaginary parts of this expression correspond to the diagonal and to the Hall component of the conductivity, respectively; $l_*=|\bar{v}_{z*}|/v$. Formula (1.5) describes the magnitude of the first (fundamental) Sondheimer signal. Figure 2 shows an experimental plot obtained by differentiating R_{xx} with respect to H

If the reflection of the electrons from the boundaries is not strictly diffuse, then σ_{osc} acquires multiple Fourier harmonics.[1)] Their amplitude differs from the fundamental only in the probability of two, three, etc. passes of the electron through the plates. Thus, allowance for the second harmonic reduces to replacing the last four factors of (1.5) by the expression

$$2^{-1/2}[\rho_d(1-\rho_0)^2+\rho_0(1-\rho_d)^2]e^{-2d/l_*}e^{2i\xi_*}, \quad (1.6a)$$

the third harmonic corresponds to

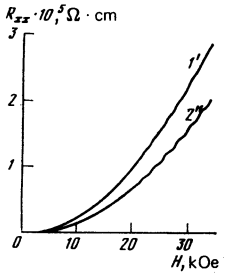

FIG. 1. Experimental plot of the diagonal component of the magnetoresistance against the field for tungsten (sample I, $d=0.095$ mm, $T=4.2$ K, $\mathbf{H}\|[100]$). Curve 1'—both sides of the plate are atomically pure, curve 2''—both sides sputtered to saturation with impurity atoms.

FIG. 2. First derivative of the magnetoresistance vs the magnetic field of sample IV ($d=1.2$ mm, $T=4.2$ K, $R_{300}/R_{4.2}=1.03$). Both sides of sample coated with a monolayer of impurity atoms.

$$3^{-1/2}\rho_0\rho_d(1-\rho_0)(1-\rho_d)e^{-3d/l_*}e^{2i\xi_*}, \qquad (1.6b)$$

etc. The numerical factors have appeared in (1.6) because with increasing number of the harmonic s the number of effective electrons that produce this signal decreases like $s^{-1/2}$ compared with (1.4). As will be shown in Sec. 2, formula (1.5) obtained by a qualitative approach, agrees apart from inessential constants with the results of the exact solution, while the factors (1.6) are quite rigorously obtained.

4. The appearance of multiple Fourier harmonics changes the form of the oscillations, but their period remains the same as before:

$$\Delta H = \frac{c}{ed}\left|\frac{\partial S_\varepsilon}{\partial p_z}\right|. \qquad (1.7)$$

The ratios of the amplitudes of the different Fourier harmonics contain the specularity coefficients and an exponential with the mean free path. This makes it possible in principle to determine these quantities from the experimental data for the group of effective electrons responsible for the Sondheimer effect.

Such a program is realized in the present paper.[2)] In the experiment we have obtained, for several tungsten samples, the oscillations of the derivative of the magnetoresistance with respect to H for different states of the crystal surface and for different temperatures. The amplitude and the waveform of the oscillations depended significantly on the concentration of the impurity atoms adsorbed by the metal surface. On the basis of the period (1.7) they could be identified with the contribution made to the conductivity by the electrons of section A on the hole octahedron of the Fermi surface of tungsten. A subsequent Fourier analysis of the Sondheimer oscillations has made it possible to determine the relations between the amplitudes of the multiple harmonics. A comparison of these quantities with the theoretical formulas has led to stable and noncontradictory results for ρ and l_*. Coating the surface of the sample with a monolayer impurity film changes the specularity coefficient in the range 0.3–0.7. The calculated mean free path l_* in these experiments turned out to be unexpectedly small ($l_* \sim 150$ μm).

2. THEORY

1. We calculate now the resistance of a plane-parallel metallic plate in a magnetic field **H** oriented perpendicular to its surface. We use a coordinate system with z axis along **H**, such that the upper and lower sides of the plate are identical with the planes $z=0$ and $z=d$. We consider a model of a metal with several groups of carriers, in which all the electron orbits in a plane perpendicular to the vector **H** are circles. In other words, all the isolated sections of the Fermi surface have axial symmetry[3)] with respect to **H**, and the electron spectrum is given by

$$\varepsilon(\mathbf{p}) = \frac{p_x^2+p_y^2}{2m(p_z)} + \varepsilon(p_z). \qquad (2.1)$$

To find the connection between the current density **j** and the electric field intensity **E**, we must use the expression

$$\mathbf{j} = -e\sum\langle \mathbf{v}\chi\rangle \qquad (2.2)$$

and the standard kinetic equation for the nonequilibrium increment χ to the electron distribution function

$$\left(\nu + v_z\frac{\partial}{\partial z} + \Omega\frac{\partial}{\partial\varphi}\right)\chi = -e\mathbf{E}\mathbf{v}. \qquad (2.3)$$

The symbol Σ denotes summation over all the carrier groups, $\Omega = eH/mc$ is the cyclotron frequency, φ is the dimensionless time of motion of the electron on the orbit, the angle brackets

$$\langle\ldots\rangle = \frac{2}{h^3}\int d\varepsilon \int dp_z |m| \oint d\varphi\,\delta(\varepsilon-\varepsilon_F)\ldots$$

denote averaging over the Fermi surface, and $h = 2\pi\hbar$.

The absence of current contacts on the surfaces $z=0$ and $z=d$ ($j_z=0$ on the boundaries), the homogeneity of the plate in the plane $z=\text{const}$, and the electroneutrality condition lead to vanishing of the normal component of the the current in the entire volume of the sample:

$$j_z = 0. \qquad (2.4)$$

It is easily seen that, because of the axial symmetry of the Fermi surface, v_z does not depend on φ and therefore (2.4) leads to the condition $E_z = 0$.

Equation (2.3) must be supplemented with boundary conditions on the surfaces $z=0$ and $z=d$. We express them in the simplest form proposed long ago by Fuchs[6]:

$$\chi^\uparrow = \rho_0\chi^\downarrow \text{ at } z=0,\ \chi^\downarrow = \rho_d\chi^\uparrow \text{ at } z=d. \qquad (2.5)$$

The first relation of (2.5) relates, via the specularity coefficient ρ_0, the anisotropic party of the distribution function of the electrons that move away from the upper boundary ($z=0$) of the plate, $\chi^\uparrow = \chi(|v_z|)$, with the function $\chi^\downarrow \equiv \chi(-|v_z|)$ for the electrons incident on the surface. The second condition in (2.5) establishes an analogous connection on the lower side of the plate, which generally speaking has a different reflection characteristic ρ_d.

The symmetry of the problem enables us to introduce the "circularly polarized" quantities

$$E_\pm = E_x \pm iE_y,$$

and to break up the distribution function into two terms, $\chi = \chi_+ + \chi_-$, which are determined from the equations

$$\left(\nu + v_z\frac{\partial}{\partial z} + \Omega\frac{\partial}{\partial\varphi}\right)\chi_\pm = -\frac{e}{2}E_\pm v_\mp. \qquad (2.6)$$

We solve them with the boundary conditions (2.5), recognizing that $v_\pm = v_\perp \exp\cdot(\pm i\varphi)$, and find

$$\begin{aligned}
\chi_\pm^\uparrow &= -\frac{e}{2\Omega}\frac{E_\pm v_\mp}{\gamma\mp i}\left[1 - N_\pm \exp\left\{-\frac{z\Omega}{|v_z|}(\gamma\mp i)\right\}\right.\\
&\quad\left.\times\left[(1-\rho_0)+\rho_0(1-\rho_d)\exp\{-\xi(\gamma\mp i)\}\right]\right],\\
\chi_\pm^\downarrow &= -\frac{e}{2\Omega}\frac{E_\pm v_\mp}{\gamma\mp i}\left[1 - N_\pm \exp\left\{-(d-z)\frac{\Omega}{|v_z|}(\gamma\mp i)\right\}\right.\\
&\quad\left.\times\left[(1-\rho_d)+\rho_d(1-\rho_0)\exp\{-\xi(\gamma\mp i)\}\right]\right].
\end{aligned} \qquad (2.7)$$

Here the function

$$N_\pm=[1-\rho_0\rho_d\exp\{-2\xi(\gamma\mp i)\}]^{-1}=\sum_{s=0}^{\infty}(\rho_0\rho_d)^s\exp\{-2s\xi(\gamma\mp i)\} \qquad (2.8)$$

determines the "number of cycles" of the periodic motion of the electrons between the boundaries of the plate, with account taken of the relative rotation of the vector $v_\perp$ and E through the angle 2ξ [Eq. (1.3)] in each of the cycles.

2. We now find the current (2.2) in the plate averaged over the thickness:

$$-\frac{e}{2}\Sigma\left\langle v_\pm\frac{1}{d}\int_0^d dz(\chi_\pm^{\downarrow}+\chi_\pm^{\uparrow})\right\rangle=\sigma_\pm E_\pm; \qquad (2.9)$$

$$\sigma_\pm=\sigma_{xx}\pm i\sigma_{yx},\ \sigma_{yy}=\sigma_{xx},\ \sigma_{yx}=-\sigma_{xy}.$$

Using (2.7) and (2.9) we obtain after elementary calculations

$$\sigma_\pm=\sigma_\pm^{\text{mon}}+\sigma_\pm^{\text{osc}},$$

$$\sigma_\pm^{\text{mon}}=\frac{2ec}{Hh^3}\Sigma\,\text{sign}\,m\int dp_z\frac{S}{\gamma\mp i}\left[1-\frac{|v_z|}{d\Omega(\gamma\mp i)}\left(1-\frac{\rho_0+\rho_d}{2}\right)\right],$$

$$+\sigma_\pm^{\text{osc}}=\left(\frac{c}{H}\right)^2\frac{2}{dh^2}\sum\int dp_z\frac{|m||v_z|S}{(\gamma\mp i)^2}\left[(1-\rho_0)(1-\rho_d)\exp\{-\xi(\gamma\mp i)\}\right.$$
$$\left.+\frac{\rho_0(1-\rho_d)^2+\rho_d(1-\rho_0)^2}{2}\exp\{-2\xi(\gamma\mp i)\}\right]N_\pm. \qquad (2.10)$$

We write down the asymptotic form of the monotonic part of the conductivity in strong magnetic fields (1.1):

$$\sigma_\pm^{\text{mon}}=\pm i(n_e-n_h)\frac{ec}{H}+\left(\frac{c}{H}\right)^2\frac{2}{h^2}\sum\int dp_z|m|S\left[\nu+\frac{|v_z|}{d}\left(1-\frac{\rho_0+\rho_d}{2}\right)\right]. \qquad (2.11)$$

We note that the last integral in (2.11) can be calculated explicitly. Indeed,

$$\frac{2}{h^3}\int dp_z|m|S|v_z|=\frac{1}{2\pi h^3}\sum_{\alpha=0}^{A+1}\text{sign}\left[\frac{\partial^2S(p_{z_\alpha})}{\partial p_z^2}\right]\int_{p_{z\alpha}}^{p_{z\alpha+1}}dp_z\frac{\partial S^2}{\partial p_z}$$
$$=\frac{1}{2\pi h^3}\sum_{\alpha=0}^{A+1}\text{sign}\left[\frac{\partial^2S(p_{z_\alpha})}{\partial p_z^2}\right][S^2(p_{z_{\alpha+1}})-S^2(p_{z_\alpha})]. \qquad (2.12)$$

Here p_{z0} and p_{zA+1} are the values of p_z on the turning points (sections) of the Fermi surface, $p_{z\alpha}(\alpha\neq0,A+1)$ are the positions of the extremal sections (their number is equal to A) where the derivative $\partial S/\partial p_z$ vanishes. The second term in the square brackets of (2.11) thus takes into account, in the monotinic conductivity, the influence of the collisions of the electrons with the boundaries and can be simply expressed in terms of the squares of the extremal sections.

We proceed now to calculate the oscillating part of $\sigma_\pm$ under the conditions (1.1) and

$$|\xi|\gg1. \qquad (2.13)$$

As already noted in the Introduction, the main contribution to the integral (2.10) with respect to p_z is made by the vicinity of points where $\xi=\xi_*$. Using the stationary-phase method and taking (2.8) into account, we obtain

$$\sigma_\pm^{\text{osc}}=-\frac{2^{1/2}}{\pi d^{1/2}h^3e^{1/2}}\left(\frac{c}{H}\right)^{1/2}\sum S_*\left|\frac{\partial S_*}{\partial p_z}\right|^2\left|\frac{\partial^2S_*}{\partial p_z^2}\right|^{-1/2}\exp\left\{\mp\frac{i\pi\beta}{4}\right\}$$
$$\times\left[(1-\rho_0)(1-\rho_d)\exp\left\{-\frac{d}{l_*}\pm i\xi_*\,\text{sign}\,m\right\}\right.$$
$$\times\Phi\left(x^2\exp\left\{\pm2i\xi_*\,\text{sign}\,m\right\},\frac{1}{2},\frac{1}{2}\right)+\frac{\rho_0(1-\rho_d)^2+\rho_d(1-\rho_0)^2}{2}$$
$$\left.\times\exp\left\{-\frac{2d}{l_*}\pm2i\xi_*\,\text{sign}\,m\right\}\Phi\left(x^2\exp\{\pm2i\xi_*\,\text{sign}\,m\},\frac{1}{2},1\right)\right]. \qquad (2.14)$$

Here

$$\beta=\text{sign}\left(m\frac{\partial^2S_*}{\partial p_z^2}\frac{\partial S_*}{\partial p_z}\right),\quad x^2=\rho_0\rho_d\exp\left(-\frac{2d}{l_*}\right), \qquad (2.15)$$

and

$$\Phi(t,n,v)=\sum_{s=0}^{\infty}(v+s)^{-n}t^s. \qquad (2.16)$$

The first term in the square brackets of (2.14) determines the contribution of the odd harmonics to the Fourier expansion, and the second only the contribution of the even ones.

3. The transverse components of the resistivity tensor $\hat{R}\equiv\hat{\sigma}^{-1}$ are expressed in terms of $\sigma_\pm$ in the form

$$R_{xx}=R_{yy}=\frac{\sigma_++\sigma_-}{2\sigma_+\sigma_-},\quad R_{yx}=-R_{xy}=\frac{\sigma_+-\sigma_-}{2i\sigma_+\sigma_-}. \qquad (2.17)$$

For a compensated metal with $n_e=n_h$ we have $\sigma_+^{\text{mon}}=\sigma_-^{\text{mon}}$, determined by the sum of the last terms of (2.11). Comparison of σ_{mon} with σ_{osc} easily shows that $\sigma_{\text{mon}}\gg|\sigma_{\text{mon}}|$ to the extent that (2.13) holds. Therefore the final formulas for the resistance can be represented in the form of an expansion in the small oscillating increment:

$$R_{xx}=R_{yy}=\frac{1}{\sigma_{\text{mon}}}\left(1-\frac{\text{Re}\,\sigma_+^{\text{osc}}}{\sigma_{\text{mon}}}\right),\quad R_{yx}^{\text{osc}}=-R_{xy}^{\text{osc}}=\frac{\text{Im}\,\sigma_+^{\text{osc}}}{\sigma_{\text{mon}}^2}. \qquad (2.18)$$

In the formulas (2.11) and (2.18) for R_{yx} we do not write out the small monontonic increments of order $\delta\sigma_\pm\sim\mp i\gamma\sigma_{\text{mon}}$ and $R_{yx}^{\text{mon}}\sim-\gamma/\sigma_{\text{mon}}$, which stem from the next terms of the expansion of the first formula (2.10) in the parameter γ.

It is also useful to have formulas for the derivatives of of the resistance with respect to the magnetic field:

$$\frac{dR_{xx}}{dH}=\frac{2}{H}R_{\text{mon}}-R_{\text{mon}}^2\text{Re}\left(\frac{d\sigma_+^{\text{osc}}}{dH}\right),$$
$$\frac{dR_{yx}^{\text{osc}}}{dH}=R_{\text{mon}}^2\text{Im}\left(\frac{d\sigma_+^{\text{osc}}}{dH}\right),\quad R_{\text{mon}}=\sigma_{\text{mon}}^{-1}. \qquad (2.19)$$

Here

$$\frac{d\sigma_+^{\text{osc}}}{dH}=-\frac{2^{3/2}c^{1/2}e^{1/2}}{d^{1/2}h^3H^{3/2}}\sum S_*\left|\frac{\partial S_*}{\partial p_z}\right|\left|\frac{\partial^2S_*}{\partial p_z^2}\right|^{-1/2}\exp\left\{i\frac{\pi}{2}\,\text{sign}\,m-i\frac{\pi\beta}{4}\right\}\cdot$$
$$\times\left[(1-\rho_0)(1-\rho_d)\exp\left\{-\frac{d}{l_*}+i\xi_*\,\text{sign}\,m\right\}\right.$$
$$\times\Phi\left(x^2\exp\{2i\xi_*\,\text{sign}\,m\},-\frac{1}{2},\frac{1}{2}\right)+\frac{\rho_0(1-\rho_d)^2+\rho_d(1-\rho_0)^2}{2}$$
$$\left.\times\exp\left\{-\frac{2d}{l_*}+2i\xi_*\,\text{sign}\,m\right\}\Phi\left(x^2\exp\left\{2i\xi_*\,\text{sign}\,m\right\},-\frac{1}{2},1\right)\right]. \qquad (2.20)$$

In (2.19) and (2.20) we have differentiated with respect to H only the rapidly oscillating functions. Formulas (2.18)–(2.20), (2.11) and (2.14) constitute the complete solution of a problem of an axially symmetrical Fermi surface.

In the general case, the oscillating derivative (2.20) describes conductivity changes that are periodic in H with a period (1.7). The oscillations of dR/dH are not harmonic, and their waveform is determined by the value of the parameter x^2 (2.15). Just as in (2.14), the first term and the brackets takes into account the odd Fourier harmonics, and the second only the even ones. If $x^2 \ll 1$ in (2.15), then the Fourier amplitudes in (2.20) decrease rapidly with increasing s. Thus, for the even harmonics the ratio of the amplitudes of the $2(s+1)$-st and 2s-th harmonics is

$$\frac{G_{2(s+1)}}{G_{2s}} = x^2\left(\frac{s+1}{s}\right)^{1/2}, \tag{2.21a}$$

for the odd ones

$$\frac{G_{2s+1}}{G_{2s-1}} = x^2\left(\frac{2s+1}{2s-1}\right)^{1/2}, \tag{2.21b}$$

and finally the ratio of G^2 and G^1 is

$$\left(\frac{G_2}{G_1}\right)^2 = \frac{x^2}{2}\left[\left(\frac{\rho_0}{\rho_d}\right)^{1/2}\frac{1-\rho_d}{1-\rho_0} + \left(\frac{\rho_d}{\rho_0}\right)^{1/2}\frac{1-\rho_0}{1-\rho_d}\right]^2. \tag{2.21c}$$

The parameter x^2 is small whenever either the mean free path is small compared with the thickness or the reflection from the boundaries is close to diffuse. To analyze the oscillations pictures convenient in this case to use the series expansion (2.16) of the functions Φ.

4. If the specularity coefficients on the opposite sides of the plate are the same, $\rho_0 = \rho_d = \rho$, then formula (2.20) simplifies to

$$\frac{d\sigma_+^{osc}}{dH} = -\frac{4c^{1/2}e^{1/2}}{\pi^{1/2}\hbar^3 H^{1/2}}\sum S_s\left|\frac{\partial S_s}{\partial p_z}\right|\left|\frac{\partial^2 S_s}{\partial p_z^2}\right|^{-1/2}$$
$$\times\exp\left\{i\frac{\pi}{2}\operatorname{sign} m - i\frac{\pi\beta}{4}\right\}\frac{(1-\rho)^2}{\rho}\Phi\left(x\exp(i\xi_s\cdot\operatorname{sign} m), -\frac{1}{2}, 0\right). \tag{2.22}$$

It is seen from this formula that the case of interest is that of sufficiently thin plates and of a nearly specular reflection ($x \to 1$). In this situation, the series in (2.22) has singularities at points $\xi_s = 2\pi k$ (k are integers). To obtain this result it is convenient to use an integral representation of the sum (2.16):

$$\Phi\left(t, -\frac{1}{2}, v\right) = \frac{1}{4\sqrt{\pi}}\int_C \frac{d\tau}{\tau^{1/2}}\frac{e^{-v\tau}}{1-te^{-\tau}}. \tag{2.23}$$

The contour C consists of the upper edge of the cut that passes along the real axis from ∞ to ε, the circle $\tau = \varepsilon e^{i\varphi}(0 \leq \varphi \leq 2\pi)$, and the lower edge of the cut from ε to ∞.

In the vicinity of the Sondheimer "resonance," when the detuning $\Delta = \xi_s - 2\pi k$ is small, we obtain

$$\Phi\left(xe^{i\xi_s}, -\frac{1}{2}, 0\right) = \frac{\pi^{1/2}}{2}[(1-x)^2+\Delta^2]^{-3/4}\exp\left\{\frac{3i}{2}\operatorname{arctg}\frac{\Delta}{1-x}\right\}. \tag{2.24}$$

In this case the waveform of the oscillations is reminiscent of bursts having a power-law singularity $dR/dH \propto |\Delta|^{-3/2}(1-\rho)^2$. In the first derivative, however, the amplitude of this effect is small because of the factor $(1-\rho)^2$. The effect begins to manifest itself most clearly in the second derivative of the magnetoresistance, for which the resonant singularity becomes stronger:

$$|d^2R/dH^2| \propto (1-\rho)^2/|\Delta|^{1/2}$$

and becomes proportional to $(1-\rho)^{-1/2}$ at the maximum.

Figure 3a shows the imaginary part of the function

$$F(x, \xi_s) = e^{-i\pi/4}\frac{(1-\rho)^2}{\rho}\Phi\left(xe^{-i\xi_s}, -\frac{1}{2}, 0\right), \tag{2.25}$$

which enters in (2.22) at $m<0, \beta=1$ and at various x. It describes the form of the periodic changes of dR_{xx}/dH. The function $\operatorname{Re}F$, which determines dR_{yx}/dH, is approximately of the same form. Figure 3b shows the derivative of $\operatorname{Im}F$ with respect to ξ_s, in terms of which d^2R_{xx}/dH^2 is expressed.

5. The results presented in this section were obtained under the assumption that the Fermi surface has axial symmetry with respect to H. Obviously, these relations are fully applicable also for the analysis of Sondheimer oscillations in anisotropic metals, if the effect is due to electrons whose orbits (in a plane perpendicular to H) are circles, and v_z does not depend on φ.

The situation can change for the effective electrons with noncircular orbits and pulsations of v_z about a mean value $\bar{v}_z$. We shall describe these changes qualitatively. It is easy to verify that if the direction of H is a rotational-symmetry axis of order r for the orbit of the electron on the Fermi surface in the plane $p_z = p_z^*$, then the velocity v has the following periodicity properties with respect to φ:

$$v_z(\varphi+2\pi/r) = v_z(\varphi), \quad v_\pm(\varphi+2\pi/r) = v_\pm(\varphi)\exp\{\pm i2\pi/r\}. \tag{2.26}$$

It follows therefore that the only nonvanishing components of the expansion of the velocity in a Fourier series in φ are those with numbers

$$kr \text{ for } v_z(\varphi),\ kr\pm1 \text{ for } v_\pm(\varphi), \tag{2.27}$$

where $k = 0, \pm1, \pm2, \ldots$

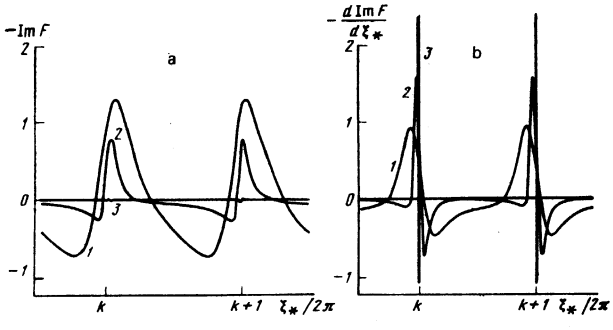

FIG. 3. Waveform of oscillations of the first derivative of the magnetoresistance dR_{xx}/dH (a) and of the second derivatives d^2R_{xx}/dH^2 (b) at different degrees of metal-boundary specularity. $\rho = x = 3, 0.7$, and 0.99 respectively for curves 1, 2, and 3.

It is quite easy to take into account noncircular motion of the electrons in a plane perpendicular to H. Formula (2.14) is in fact the contribution made to $\sigma_{\pm}^{osc}$ by the Fourier components of the velocity $v_{\pm}(\varphi)$ with $k=0$. The components with $k\neq 0$ yield additive corrections to the conductivity. An expression for the k-th term can be obtained from (2.14) by the formal substitution $\pm i \to i(kr \pm 1)$. In addition, this expression is proportional not to S_* but to $m^2|kr\pm 1|^{-1/2}$ and to the square of the modulus of the k-th Fourier component of the velocity, i.e., to $|v^{\pm}_{kr\pm 1}|^2$. It can be furthermore found that for noncircular orbits the amplitudes G of all the higher Fourier harmonics of the Sondheimer signal experience a small change (relative to the parameter $|v^{\pm}_{kr\pm 1}/v_F|^2$). The only exceptions are those G_s whose numbers are represented by powers of two, $s=2,4,8,16,\ldots$. For these G_s (as also for $s=1$) all the formulas written out above remain valid.

The question of the dependence of v_z on φ is much more complicated. The reason is that in coordinate space these electrons drift on the average along H and execute reciprocating motion. Even if $\bar{v}_z=0$, their trajectories can be nonplanar. From the mathematical point of view, this recalls the problem of the motion of an electron in a plate in a magnetic field parallel to the surface. However, even in this situation it is possible to formulate a criterion sufficient for the validity of the theory developed above. Thus, if the amplitudes of the Fourier components of the velocity v_z are small compared with $\bar{v}_z$ to such an extent that when an electron moves from one side of the plate to the other the sign of v_z is not reversed, then the period of the oscillations is given as before by formula (1.7). In the opposite case, when the pulsations of v_z are relatively large, new periods may appear in the Sondheimer signal. Thus, the dependence of v_z on φ does not influence the ratio of the amplitudes of the multiple Fourier harmonics. An investigation of the Sondheimer effect in metals with a complicated Fermi surface is an independent problem.

3. EXPERIMENTAL RESULTS AND THEIR DISCUSSION

1. We measured in the experiment the transverse magneto-resistance of single-crystal plates of tungsten. The sample thickness and the ratio of the resistance at room and helium temperatures $R_{300K}/R_{4,2K}$ (certified nominal data), which characterizes the quality of the initial material, are listed in the summary table. The initial cleaning of the metal surface was carried out in vacuum by standard procedure.[7] In the course of the experiment it was possible to vary the state of the crystal surface in controlled fashion. This was done by sputtering on the sides of the plate in vacuum (10^{-11} Torr) a monolayer film of impurity atoms.

The impurity source was located inside the experimental tube and constituted a tungsten filament of 150 μm diameter. The filament surface always contained some amount of gas (apparently CO) that settled from the residual gas. Atmosphere by heating the filament, the gas was desorbed and settled on the surface of the crystal. The surfaces was subsequently cleaned by heating the sample to a temperature 2500 K.

The experimental material consisted of plots of the diagonal component of the magnetoresistance R_{xx} and of its derivative dR_{xx}/dH against H. The measurements were performed in a superconducting solenoid in fields up to 32 kOe. We used a standard modulation procedure to plot the derivative of the resistance. The amplitude of the modulation of the magnetic field was 20–30 Oe and the frequency was 36 Hz. At this frequency, the depth of the skin layer is of the order of $\delta(\text{cm}) \sim 10^{-4}$ H (Oe) and is larger than the thickest of the employed samples in a field of several kilooersted. Figure 4 shows a general diagram of the experimental tube, the geometry of the experiment, and a schematic representation of the Fermi surface of tungsten.

2. The first group of the experimental data pertains to the monotonic function $R_{xx}(H)$. Figure 5a shows a plot of $R_{xx}(H)$ for the sample W III with different surface states. The first curve 1′ corresponds to a crystal with both surfaces atomically clean (we shall henceforth call them "clean" and mark them with a single prime). The sequence of curves 2‴ and 3‴ demonstrates the decrease of R with increasing concentration of the impurities on one side of the plate. The lower curve 4″ was obtained for a plate with both surfaces sputtered to saturation (henceforth called "dirty"—double prime). After recording this family of curves it was possible to return the crystal to the initial state by heating, and repeat the entire sequence of experiments. Figure 5b illustrates the dependence of R on the temperature in the limiting cases of clean surfaces (curves 5′ and 1′) and dirty surfaces (6″ and 4″). The upper curve of each pairs corresponds to $T=2.25$ K and the lower to $T=4.2$ K.

Figures 1 and 5 attest to the quadratic dependence of R_{xx} on the magnetic field (the plots against H^2 are straight lines) in all the investigated methods of sputtering the surfaces and for all temperatures. Increasing the tem-

TABLE I. Summary experimental data obtained for tungsten samples*

Sample	T, K	d, mm	$\frac{R_{300}\cdot 10^{-3}}{R_{4,2}}$	$\frac{R_{\text{mon}}}{R''_{\text{mon}}}$	$\frac{G'_1}{G''_1}$	$\frac{G_1'}{G_2'}$	$\frac{G_1''}{G_2''}$	$\frac{G_1'}{G_3'}$	$\frac{G_1''}{G_3''}$	$\frac{G_1'}{G_4'}$	$\frac{G_1''}{G_4''}$	ρ'	ρ''	l, mm
WI	4.2	0.095	0.95	1.1	0.24	3.4	6.9	15.7	38.5	—	—	0.75	0.39	0.073
WII	4.2	0.161	1.03	1.3	0.34	2.62	7.0	10.5	18.1	22.2	37.9	0.65	0.24	0.18
WIII	2.15	0.161	—	1.6	0.35	3.57	9.43	17.6	37.3	—	—	0.73	0.28	0.12
	4.2	0.161	—	1.6	0.37	3.48	8.68	—	—	—	—	0.74	0.30	0.12

*Samples W II and W III are in fact the same crystal, whose kinetic characteristics were altered in the course of the high-temperature treatment.

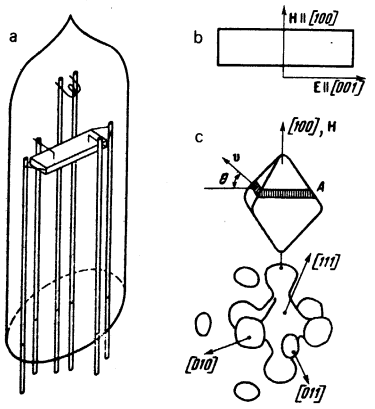

FIG. 4. Experimental vacuum tube (a), geometry of experiment (b), and Fermi surface of tungsten (c).

perature and the concentration of the adsorbed atoms decreases the resistance. These relations agree fully with formula (2.11), which was experimentally confirmed with approximate accuracy 5% (see below). It was noted in Sec. 2 that expression (2.18) describes the oscillations of the Hall component of the magneto-resistance R_{yx} with a small monotonic part $R_{yx}^{mon} \sim -\gamma/\sigma_{mon} \propto H$. At first glance this statement contradicts the experimental data of Soule and Abele.[8] They investigated R_{xx} and R_{yx} in tungsten in the same geometry as in our experiment. The results of Soule and Abele on R_{xx} agree fully with the conclusions of the present paper. Their data for the Hall resistance consist in the following. In absolute magnitude, R_{yx} is smaller by one order of magnitude than R_{xx} and the curves show, in addition to the oscillations, a growth, approximately quadratic in H, of the monotonic part of R_{yx}. In our opinion this result is due to the fact that the potential Hall contacts were not perpendicular to the direction of the electric current, and reflects the exceeding sensitivity of the Hall measurements to the geometry of the experiment. In fact, $|R_{yx}^{mon}|/R_{xx} \sim \gamma \ll 1$. This means that the angle error ϕ in the experiment causes the measured quantity to be not R_{yx} but the combination $R_{yx} + \phi R_{xx}$. Favoring this argument is also the fact that the ratio R_{yx}^{osc}/R_{mon} in "Hall" geometry[8] greatly exceeds the relative amplitude R_{xx}^{osc}, which, judging from the formulas, should indeed be smaller than the Hall amplitude by a factor ϕ^{-1}. The limitation on the angle ϕ in the Hall measurements is quite stringent: $\phi \ll \gamma \ll 1$.

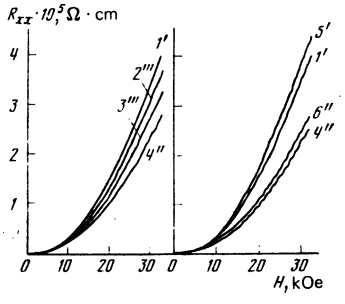

FIG. 5. $R_{xx}(H)$ plot for sample III. Left—effect of plate soiling: temperature 4.2 K, curve 1′—both sides of plate clean, 2‴ and 3‴—successive increase of impurity concentration on one side of the plate, 4″—both surfaces sputtered to saturation. Right—effect of temperature on plate resistance: curves 5′ and 6″ correspond to $T = 21.5$ K, curves 1′ and 4″ to $T = 4.2$ K.

In addition to the $R_{xx} \propto H^2$ law, expression (2.11) describes the dependence of the resistance on the thickness d. Figure 6 shows a plot of $R_{xx}(d)$ at a fixed value of H, constructed from the data of Ref. 9. According to (2.11), at small thicknesses R_{xx} increases linearly with d, this being due to a decrease in the contribution of the surface mechanism of the electron scattering. For thick crystals, the resistance saturates at a level determined by the resistivity of the bulk sample. Formula (2.11) contains the contributions made to the monotonic part of the conductivity by electrons of various groups, for which the specularity coefficients are generally speaking not the same. Nevertheless, it has one curious property. It is easy to verify that (2.11) leads directly to the following universal relation:

$$R_{xx}'/R_{xx}'' + 1 = 2R_{xx}'/R_{xx}''', \tag{3.1}$$

where R' is the resistance of the close plate, R'' is the resistance with both sides dirty, and R''' is the resistance with one clean and one dirty side. This relation was verified for two samples, W I and W III. It was found that it is satisfied with relative accuracy 2% in the former case and about 5% in the latter. A change of the reflecting ability of the surface of the metal leads to variation of the monotonic resistance by an amount of the order of 40%. This follows from the ratio R'/R'' listed in the table.

3. The next set of experimental results describes the oscillations of $R_{xx}(H)$. As seen from Figs. 1 and 5, their amplitude is small, so that it is simpler to investigate them with the aid of the derivative dR_{xx}/dH. By way of example, Fig. 7 shows an automatic plot of the derivative obtained for sample W II. The upper curve represents oscillations on atomically clean surface, and the lower on dirty ones. This plot is described by the first formula of (2.19). Its first term gives the course of the monotonic part of dR_{xx}/dH, which increases linearly with H, while the second term gives the Sondheimer oscillations. On all the experimentally observed curves, the period of the oscillations did not depend on the magnetic field. From (1.7) we obtained the quantity

$$\frac{1}{2\pi\hbar}\left|\frac{\partial S_z}{\partial p_z}\right| = 0{,}492\ \text{Å}^{-1}, \tag{3.2}$$

which made it possible to relate the group of electrons that manifested themselves by the oscillations to section A of the hole octahedron of the Fermi surface of

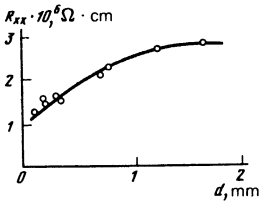

FIG. 6. Resistance of tungsten plate vs its thickness at a fixed $H = 10$ kOE ($\mathbf{H} \parallel [100]$, $T = 4.2$ K).

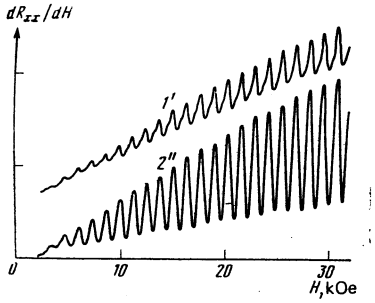

FIG. 7. Plot of the derivative of the magnetoresistance against the magnetic field at sample II ($d = 0.6$ mm, $T = 4.2$ K) with clean (curve 1') and dirty (2'') sides.

tungsten. The value (3.2) agrees with the data on the radio-frequency size effect is tungsten.

It is seen from Fig. 7 that the amplitude of the oscillations is larger on a dirty surface than on a clean one. This is due to the appreciable decrease of the specularity coefficient when the crystal surface is coated. When the surface is cleaned the decrease of the amplitude is accompanied by a change of the form of the oscillations. We attribute it to the appearance of multiple harmonics of the Sondheimer signal. They result from multiple passage of the electron through the particle, if the angle ξ [Eq. (1.3)] of its collision with the boundary is preserved. For a direct proof and for a quantitative description of the multiple Sondheimer effect, the oscillating part of dR_{xx}/dH, of each experimental plot was Fourier-analyzed; an example is shown in Fig. 8. It is clearly seen that with decreasing concentration of the adsorbed impurity atoms the amplitudes of the multiple harmonics relative to G_1 increase. This regularity is reflected in the results of the Fourier analysis of all the experiments, which are also shown in the table (columns 6 – 12).

4. Now, using Eqs. (2.21) and the experimental relations for the amplitudes G from the table, we can proceed to a direct calculation of the mean free path l_* of the resonant electrons, of the specularity coefficients of clean (ρ') and dirty (ρ'') surfaces of the crystal. If both sides of the plate reflect the electrons in like manner, than the ratio of the amplitudes of the second and first harmonics in (2.21) simplifies noticeably:

$$G_2/G_1 = \sqrt{2}\rho e^{-d/l_*}. \tag{3.3}$$

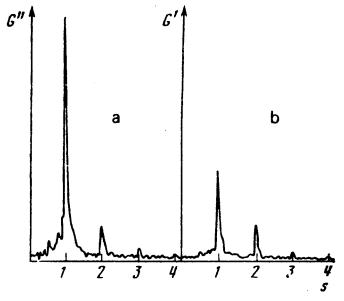

FIG. 8. Dependence of the amplitudes G_s of the Fourier harmonics on the number s for the oscillation curves 2'' (a) and 1'' (b) of Fig. 7.

Combining the amplitude G' and G'', we can eliminate from the formula the exponential with the mean free path

$$\rho' = \rho'' G_1'' G_2' / G_1' G_2''. \tag{3.4}$$

We compare next the amplitudes from the different Fourier spectra. With the aid of (2.19) and (2.22) we easily obtain

$$\frac{G_1''}{G_1'} = \left(\frac{R_{\text{mon}}''}{R_{\text{mon}}'} \frac{1-\rho''}{1-\rho'} \right)^2. \tag{3.5}$$

In the comparison of experiment with theory we purposely use the ratios of the amplitudes of the first two Fourier harmonics. For these harmonics the signal-to-noise ratio, as seen from Fig. 7, is much higher than for the higher harmonics (see also item 5 of Sec. 2). The three formulas (3.3)–(3.5) allow us to express in terms of the observable characteristics the three sought quantities:

$$\rho'' = \frac{1 - (R_{\text{mon}}'/R_{\text{mon}}'')(G_1''/G_1')^{1/2}}{1 - (R_{\text{mon}}'/R_{\text{mon}}'')(G_1''/G_1')^{1/2}(G_2'/G_2'')}, \qquad l_* = d/\ln(\sqrt{2}\rho G_1/G_2) \tag{3.6}$$

and ρ' from (3.4). With the aid of these working relations we calculated ρ', ρ'', and l_* for each sample. They are given in the last three columns of the table.

There are several methods of checking the validity of the formulas used by us to reduce the experimental data. Thus, for example, from (2.22) and (3.3) we can express in terms of G_1 and G_2 the amplitudes of the higher harmonics:

$$\frac{G_3}{G_1} = \frac{\sqrt{3}}{2}\left(\frac{G_2}{G_1}\right)^2, \quad \frac{G_4}{G_1} = \frac{1}{\sqrt{2}}\left(\frac{G_2}{G_1}\right)^3, \ldots \tag{3.7}$$

A comparison of these relations with the experimental results from the table shows that they are satisfied with a relative accuracy of the order of 40%.

5. It must be borne in mind that the geometric imperfection of the sample, just as the finite mean free path, can decrease the amplitude of the Sondheimer oscillations. The whole point is that the uncertainity δd of the plate thickness produces in the angle ξ_* a scatter amounting to $\delta\xi_* \sim \xi_* \delta d/d$. This dephasing of the electrons decreases strongly the oscillating signal. This effect can be taken into account in order of magnitude by making the substitution $d \to d + i|\delta d|$ in formula (1.3) for ξ_*. Then σ_{osc} turns out to be

$$\sigma_{\text{osc}} \propto \exp\left\{-\frac{d}{l_*} - \frac{|\delta d|}{d}\xi_*\right\} \exp\{i\xi_*\}.$$

Now l_*^{-1} in all the formulas will be replaced by

$$l_{\text{eff}}^{-1} = l_*^{-1} + \xi_* |\delta d|/d^2. \tag{3.8}$$

With increasing H the role of the additional term in (3.8) increases ($\xi_* \sim H$), and further decrease of the effective mean free path $l_{\text{eff}} \propto H^{-1}$ can cause the oscillation amplitude to decrease in very strong fields. Estimates show that in our experiments the decisive quan-

tity in l_{eff} was l_*. Thus, if the sample finish was accurate to $|\delta d| \sim 1$ μm, the second term in (3.8) is smaller than the reciprocal mean free path ($l_* \sim 150$ μm) even for the thinnest sample, W I ($d \sim 100$ μm) and in the strongest fields ($\xi_* \sim 20$).

4. CONCLUSIONS

1. We have quantitatively estimated the absolute value and the change of the coefficient of specular reflection of electrons by a metal surface. The basis for the calculations was the Fuchs model (2.5), which is fully analogous to the τ-approximation in kinetic theory. The noncontradictory character and the stability of our results show that this model is not only simple but also representative of the phenomena that occur on a metal boundary. We note that the assumption used above, that the coefficient ρ is constant, is not obligatory. All the arguments and results for the oscillating part of the resistance remain valid also if ρ is a slowly varying function of the incidence angle ϑ of the electrons on the metal surface (ϑ dpends in turn on p_z). More accurately speaking, the interval over which ρ changes must be wider than δp_z given by (1.4). This is the condition that all the electrons on the effective section be reflected from the boundary in like fashion. Bearing this remark in mind, ρ must be taken to mean the quantity $\rho(\vartheta_*)$, equal to the coefficient of specular reflection of the electrons from a given effective group from the metal surface.[4)]

Our experiments and the comparison with the conclusions of the theory demonstrate quite convincingly that it is possible to obtain on the (100) face of tungsten a sufficiently high degree of specularity for the electrons responsible for the Sondheimer effect. The sample sputtering technology used in the described experiments makes it possible to vary the specularity coefficinet in a wide range from $\rho'' \sim 0.3$ to $\rho' \approx 0.7$. It is interesting that even at the maximum impurity concentration, when the entire surface of the crystal is covered by a solid film of adsorbed atoms, the reflection coefficient of the effective electrons is quite high, $\rho'' \approx 0.3$.

2. It was already noted at the end of Sec. 2 that if the effective electrons have noncircular orbits, then the relations (2.21) between the amplitudes of the higher Fourier harmonics (with $s > 2$) are somewhat modified. This circumstance complicates the analysis of the experiment because of the appearance of new unknowns, namely the Fourier components of the transverse velocity of the electron. However, even in this case, if the experimental spectrum of the oscillating signal contains several (up to five) well resolved and high maxima, it is possible to formulate a straightforward (albeit unwieldy) program with which toe determine, besides ρ and l_* also the quantities $|v^{\pm}_{kr\pm1}|^2$. In other words, a possibility exists of reconstructing the forms of the effective sections on the Fermi surface.

3. Attention must be called to another, perhaps most important result of the present paper. Even though we used in our experiments very pure tungsten samples, the calculated mean free paths l_* turned out to be unexpectedly small ($l_* \sim 150$ μm). The possible reason is that the length l_* characterises only a narrow layer of sections near p_z^*. It is therefore determined by the departure relaxation time, and not by the transport time as is the mean free path l in the monotonic part of the resistance. If the electrons are scattered through a small angle, then this can lead to values of l_* much smaller than the transport mean free path. Favoring the small length l_* are also the data of a volume effect—the Doppler-shifted cyclotron resonance of ultrasound in tungsten and in molybdenum[11] (the surfaces of the hole octahedron practically coincide in these metals). In these experiments the resonance on the section A takes the form of a broad and low maximum (smeared-out step), whereas the other groups of electrons are manifest by sharp and high peaks in the sound absorption. An alternate explanation of the short mean free path is the following. The length that enters in the size effect can not be the tree mean free path of the effective electrons in a bulky metal, and is determined by the surface electron-scattering mechanisms. In this case the calculated value of l_* must coincide in order of magnitude with the sample thickness d (see the table). The question of the mean free path determined from the size effect is not clear to this day and calls for additional research.

We note in conclusion that the procedure described in the paper is a convenient method of determining the reflecting properties of a metal boundary for electrons of a given group singled out by the Sondhemier effect. It offers much information, since it makes it possible to to determine in a single experiment a large number of characteristics, and identifies at the same time the group of particles that are responsible for the effect. This method may be particularly promising in studies of the effect of the surface-finish method and of the sort of atoms adsorbed by the boundary on the specularity coefficient.

The authors are deeply grateful to É. A. Kaner for numerous discussions during all stages of the work, and A. S. Kharlamov for help with the preparation of the samples.

1) The appearance of additional resistance oscillations was first predicted by Goland.[4]
2) The first results were published by us earlier.[2)]
3) At the end of Sec. 2 we discuss the effect of lowering the surface symmetry on the final results.
4) A simple examination of the pictures of the Fermi surface of tungsten (see, e.g., the figure in Ref. 8 or Fig. 4c) permits a rough estimate of the incudence angle $\vartheta = \tan^{-1}(v_z/p_\perp)$ of the electrons of section A on the metal surface. It is found to be $\vartheta_* \sim 35°$.

[1]R. Chambers, in: Physics of Metals, 1. Electrons, J. M. Ziman, ed., Cambridge U. Press, 1969.
[2]E. H. Sondheimer, Phys. Rev. **80**, 401 (1950).
[3]V. L. Gurevich, Zh. Eksp. Teor. Fiz. **35**, 668 (1958) [Sov. Phys. JETP **8**, 464 (1959)].
[4]Yu. M. Goland, Fiz. Tverd. Tela (Leningrad) **10**, 81 (1968) [Sov. Phys. JETP **10**, 58 (1968)].
[5]A. M. Grishin, Yu. S. Ostroukhov, and O. A. Panchenko, Abstracts of Papers NT-19, M-19, Minsk, 1976.
[6]K. Fuchs, Proc. Cambridge Philos. Soc. **34**, 100 (1938).
[7]J. A. Becker, E. J. Becker, and R. G. Brandes, J. Appl. Phys.

32, 411 (1961).
[8]D. E. Soule and J. C. Abele, Phys. Rev. Lett. **23**, 1287 (1969).
[9]O. A. Panchenko and P. P. Lutsishin, Zh. Eksp. Teor. Fiz. **57**, 1555 (1969) [Sov. Phys. JETP **30**, 841 (1970)].
[10]I. M. Vitebskiĭ, V. T. Vitchinskiĭ, A. A. Galkin, Yu. S. Ostroukhov, O. A. Panchenko, L. T. Tsymtal, and A. N. Cherkasov, Fiz. Nizk. Temp. **1**, 400 (1975) [Sov. J. Low Temp. Phys. **1**, 200 (1975)].
[11]A. A. Galkin, L. T. Tsymbal, A. M. Grishin, and T. F. Butenko, Pis'ma Zh. Eksp. Teor. Fiz. **25**, 98 (1977) [JETP Lett. **25**, 87 (1977)].

Translated by J. G. Adashko

Nonstationary Josephson effect at a point junction under high voltage

Kh. A. Aĭnitdinov, S. I. Borovitskiĭ, and L. L. Malinovskiĭ

(Submitted 22 Septebmer 1978)
Zh. Eksp. Teor. Fiz. **76**, 1342–1350 (April 1979)

The behavior of the Josephson current steps observed at high microwave potentials and powers in the case of a new type of clamped point junction is explained. It is concluded that at junctions consisting of metallic bridges which are small (of size d) compared with the coherence length (ξ_0) and mean free path (l), the phase dependence of the nonstationary Josephson current is sinusoidal. The formation of the current step is restricted by the heating of the junction at high voltages. The limiting voltage is $V_h \sim (l/d)^{1/2}$. For the Nb–Nb junctions studied, Josephson steps up to 14 mV have been obtained.

PACS numbers: 74.50. + r, 85.25. + k

INTRODUCTION

At a voltage above the energy gap of a superconductor $eV > 2\Delta_0$, the nonstationary Josephson effect at tunnel junctions has been observed experimentally by Hamilton[1] and described theoretically by Werthamer[2] and by Larkin and Ovchinnikov.[3] The height of the current step induced by microwaves was calculated earlier.[4] The most remote steps in voltage at a tunnel junction have been observed by McDonald *et al.*[5] No description has been made of the behavior of point junctions at voltages beyond the gap value, although there is interest both in the theory and in the practical utilization (for example, as a voltage standard).

In the present work we set forth the results of an experimental study of the characteristics of a clamped Josephson point junction of a new type in a microwave field, and explain it on the basis of a proposed microscopic theory of a bridge of dimensions less than $\{l, \xi_0\}$. From a comparison of the measured dependence of the height of the induced steps on the microwave amplitude with the theoretical value, it is concluded that the phase of the nonstationary Josephson current has a sinusoidal dependence on the phase in the investigated junctions. The dependence of the current step height I_N at the upper voltage limit on its value V_N has an asymptotic form: $I_N(V_N) \sim V_N^{-1/3}$. Preliminary results of the research were reported earlier.[6]

DESCRIPTION OF THE JUNCTION

The experiments were carried out with clamped Nb–Nb junctions, which were prepared under room conditions and which did not change their characteristics after numerous coolings to the temperature of liquid helium ($T = 4.2$ K). The junction shown schematically in Fig. 1 comprises a wire electrode in the form of a loop pressed to a flat electrode. The flat screen-electron was made of single-crystal Nb and its surface was carefully smoothed by electrochemical polishing. The surface of the niobium loop was cleansed from foreign impurities and oxides by chemical etching.

A trace of the loop with overall dimension 5×100 μ is seen on a microphotograph of the screen, obtained by means of a scanning electron microscope after dismantling the junction. It can be assumed that a set of microbridges is formed on this area, distributed in correspondence with the very inhomogeneous microstructure of the wire surface. The total resistance of the junction is the combination of the resistances of the microbridges connected in parallel.

In correspondence with this model, the average diameter of the microbridges was determined from the measurements of the dependence of the resistance of the junction on the temperature $R(T)$ and voltage $R(\bar{V})$. The measurement of $R(T)$ and $R(\bar{V})$ was carried out in a thermostat in which the temperature was maintained and measured accurate to ~1 in the range 12–300 K. The dependence $R(\bar{V}) = d\bar{V}/d\bar{I}$ was determined from the value $\bar{V} - \bar{I}R(0)$, measured with the help of a bridge

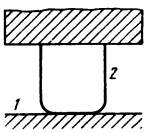

FIG. 1. Schematic diagram of the clamped point Josephson junction of the new type: 1—plane electrode-screen, 2—wire electrode-loop.

 0038-5646/79/040682-06$02.40